



# Mechanical and biocompatibility properties of UHMWPE–HNT composite for joint replacement applications

LANIA HASAN<sup>1</sup>, SARANG PANDE<sup>1,\*</sup>  and PRAVIN BHALERAO<sup>2</sup>

<sup>1</sup>Department of Mechanical Engineering, Marwadi University, Rajkot 360003, India

<sup>2</sup>Department of Chemistry, Marwadi University, Rajkot 360003, India

\*Author for correspondence (sarang.pande@marwadieducation.edu.in)

MS received 23 January 2024; accepted 16 April 2024

**Abstract.** Ultrahigh molecular-weight polyethylene (UHMWPE)-based composites are extensively utilized as a bearing surface in joint replacements. In the present study, due to their unique and versatile attributes halloysite nanotubes (HNTs) were used as additives in different percentages 1, 3, 5, 7 and 10 wt% to enhance the properties of UHMWPE. The effects of the weight fraction of HNT on UHMWP were investigated in terms of hardness, abrasion strength, compression strength, bulk modulus, impact resistance and biocompatibility, and the specimen showed that only a small amount of HNT (1%) optimized all the mentioned properties by 26.8, 20.77, 174.7, 351.53, 11.35 and 95%, respectively. The percentage of 5% HNT achieved the optimal content, at which the composites experienced the maximum enhancement for compression, abrasion and hardness properties. *In-vitro* MTT assay of UHMWPE with 1, 3 and 5% HNT nanocomposites using MG-63 cells revealed high cell viability (94.307%) after 4 days of incubation in media at concentrations of 100, 50 and 25  $\mu\text{g ml}^{-1}$ , indicating excellent biocompatibility. These results might lay a solid basis for load bearings used in orthopaedic applications of UHMWPE-based composites.

**Keywords.** UHMWPE; HNT; compression test; biocompatibility; load bearing.

## 1. Introduction

Nowadays, joint replacements are recognized as among the most successful surgical procedures, primarily due to their efficacy in treating challenging diseases, including osteoarthritis, rheumatoid arthritis, hip fractures and tumours that cause persistent pains [1]. Biocomposite materials have gained significant attention over traditional materials as promising orthopaedic biomaterials, due to their capacity to manipulate biological and mechanical properties across a broad range by customizing the reinforcing components and altering the degree of filling in a controlled manner [2,3]. These materials can be categorized as either micro or nano-composites, based on the size of the filler utilized. The rapid development of nanotechnology has granted superior progress in synthesizing highly advanced nanocomposites for various applications, especially in the field of functional biomedical [4]. In this context, the exceptional attributes of ultrahigh molecular-weight polyethylene (UHMWPE), which meet the primary mechanical and biological demands, such as low coefficient of friction, wear resistance, chemical stability, good abrasion resistance and toughness have made UHMWPE a successful matrix to be used as a load-bearing material in orthopaedic applications [5,6]. One restriction of current UHMWPE components in total joint arthroplasty is their

limited thickness, as they can potentially fracture under the high stresses raised, especially when used as one of the components of the acetabular cup in hip implants or as a bearing surface in the knee, ankle, shoulder and as a prosthetic cruciate ligament [6]. At the same time, the low bulk modulus and hardness may critically constrain its suitability for various applications [7,8].

Based on recent literature, the use of nano-reinforced UHMWPE composites meets the growing need to enhance the tribological and mechanical properties of UHMWPE, for use as potential replacements in orthopaedic prostheses. Thus, a strong interest in the development of UHMWPE-based nanocomposites emerged for enhancing mechanical strength without compromising other outstanding properties, like wear resistance, lubricity and biocompatibility [9–14]. Since the biomechanical properties of synthetic composites should appear to have a microstructure comparable to natural bone, hydroxyapatite (HA)-reinforced UHMWPE was introduced to combine the preferable toughness of UHMWPE with the high stiffness of HA [15,16].

Graphene has generated significant attention as a filler to boost polymeric substrates and polymer matrix, optimizing the mechanical and tribological features of composites [17–19]. Carbon nanotubes (CNTs) have also been used to strengthen polymer-based composites, especially in the field

of biomedical implants. Different factors, such as cylinders of one or several graphene layers single-wall SWCNT or multi-wall MWCNT, different lengths, open or closed ends, purity, and structural defects, might influence the final feature of CNTs composites. These composites successfully achieved good mechanical properties for small percentages of CNT and higher contents led to a minor degree of enhancement [17,20]. However, despite their novel features, carbon-based nanomaterials have reported the potential toxicity to cell growth. Consequently, queries persist regarding their biocompatibility and resulting biological responses in the field of biomedical applications [21–23].

As a natural nanofiller, halloysite nanotube (HNT), whether as it is or after its modification, has attracted significant attention in the 21st century due to its inexpensive cost, exceptional mechanical, thermal and biological properties, and achieving mechanical improvement that is equivalent to that of CNTs [24,25]. HNTs as a two-layered aluminosilicate, belong to the kaolin group and are geometrically similar to CNT hollow tubular form with a porous inner surface that gives the potential to carry both chemical- and biological-active agents [24–26]. Additionally, HNT is a non-toxic filler and could offer adjustable release rates, rendering it a well-suited choice for biomedical applications [27–29]. Although HNTs have been effectively used to reinforce many polymers, no report to be introduced as nanofillers for reinforcing with UHMWPE to form nanocomposite materials that can be load bearings in artificial joint implants.

## 2. Experimental

In this study, the primary powders have been compacted by compression moulding approach and two-roll mill with different percentages of HNT, such as 1, 3, 5, 7 and 10% to prepare UHMWPE/HNT nanocomposites. Since the mass fractions of nanofiller influence the ultimate feature of the material, we have carefully chosen HNT content at both low loading (<5%) and high loading (>5%) of HNT to achieve the best possible mechanical properties in fabricated UHMWPE/HNT nanocomposite. Our study focuses on developing load-bearing components for bone replacement nanocomposite. The experimental evaluation involved hardness, abrasion, the Izod impact test, a compression test and biocompatibility through MTT assay testing, which address the basic requirement to handle body weight and strenuous activities.

### 2.1 Materials

The UHMWPE (POLIMAXX U511) powder was obtained from IRPC Public Company Limited, with an average molecular weight of about 5.5 million  $\text{g mol}^{-1}$  and the size

of the particles 140  $\mu\text{m}$ . HNT nanopowder was from Sigma-Aldrich, with diameter  $\times$  length 30–70 nm  $\times$  1–3  $\mu\text{m}$ , and surface area 64  $\text{m}^2 \text{g}^{-1}$ . To improve the interfacial adhesion and optimize the miscibility of UHMWPE with HNT, maleic anhydride (MA) has been used as a compatibilizer.

### 2.2 Fabrication of UHMWPE/HNT nanocomposite

The processing and compounding steps of both Pure UHMWPE and UHMWPE/HNT nanocomposites have been shown in figure 1. Initially, the nanocomposites were prepared by mixing 1, 3, 5, 7, 10 wt% of HNT and 5 wt% MA compatibilizer to UHMWPE. Due to the high viscosity of UHMWPE, particularly when mixed with other materials, on a two-roll mill, the rolling process is carried out at a temperature 35°C below the actual melting point (135°C) of the UHMWPE for 15 min, with the rolls rotating at a speed of 10 rpm. Rolling changed the shape of the powder into thin flakes; shear forces generated reduced UHMWPE viscosity and ensured uniform dispersion of HNT and MA in the matrix. The flattened flakes were placed in two pre-heated stainless-steel moulds at 160°C, and 150  $\text{kg cm}^{-2}$  pressure was applied for 5 min to shape these flakes; then hot pressing applied for 10 min at 190°C, 300  $\text{kg cm}^{-2}$  to form sheets 25  $\times$  20  $\times$  3.2 mm, and 220°C, 300  $\text{kg cm}^{-2}$  to form a rectangular shape. A cooling process to room temperature subsequently occurred under the same 300  $\text{kg cm}^{-2}$  pressure. Pure UHMWPE samples were also prepared by a similar method but in the absence of HNT and MA compatibilizers.

### 2.3 In-vitro biocompatibility investigation

Osteoblasts (MG-63 cell line) were used for *in-vitro* biocompatibility valuation of UHMWPE/1,3,5% HNT nanocomposites and assessing the cell viability. MG-63 cells were cultivated and maintained to grow (forming a monolayer at sub-confluent conditions) in a nutrient medium comprising minimum essential medium (MEM) w/ Earle's salts, 2 mM L-glutamine, 1 mM sodium pyruvate, non-essential amino acid and 1.5  $\text{g l}^{-1}$  sodium bicarbonate with 10% foetal bovine serum. Cultivation occurred in a humidified incubator at 37°C with 5%  $\text{CO}_2$ . The continuous passage was achieved by trypsinizing sub-confluent cultures using a TPVG solution. In the subsequent stage, the stock solution created three primary working solutions (100, 50 and 25  $\text{mg l}^{-1}$ ). This latter was prepared by dissolving 10 mg of pure UHMWPE and UHMWPE+ (1, 5, 10%) HNT nanocomposite in 10 ml of cell-cultured-grade dimethyl sulphoxide (DMSO), followed by sterile filtration and sterilization. Following that, the MTT assay, which is a widely used cytotoxicity test for assessing cell viability and proliferation, was performed. This test involved seeding

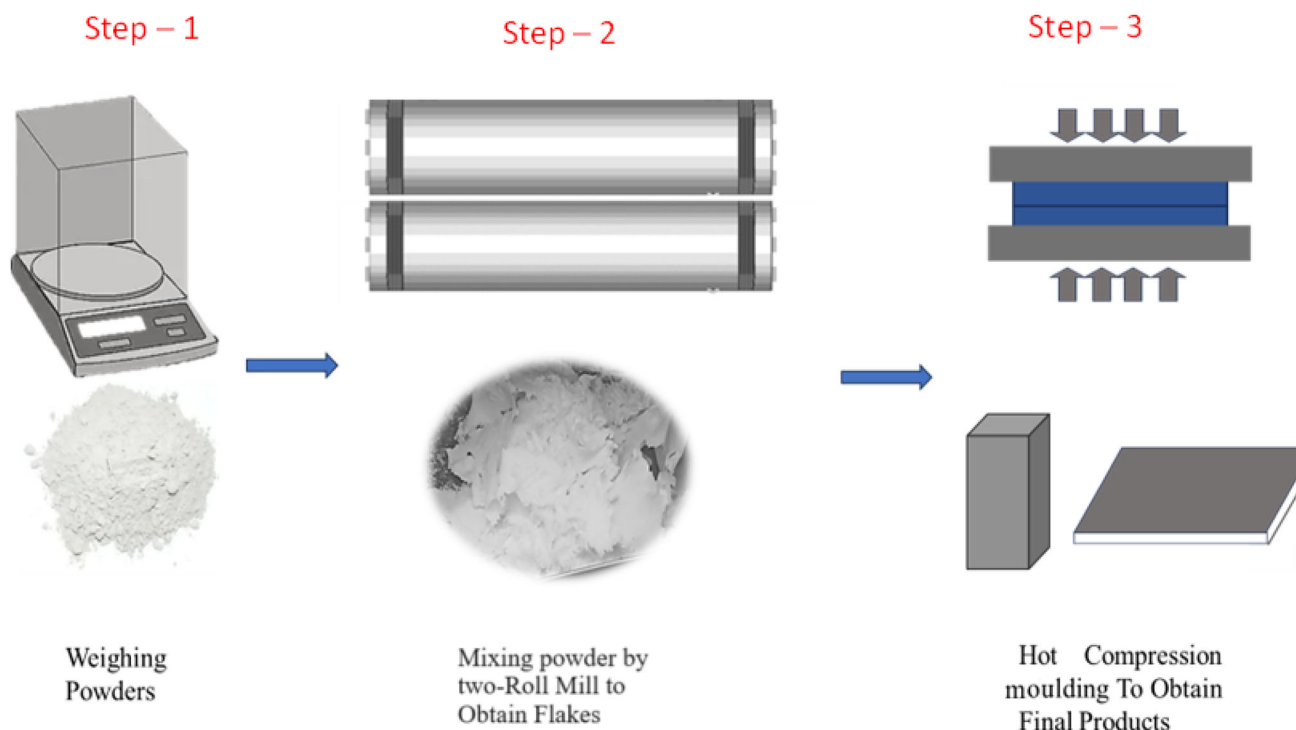


**Figure 1.** Schematic representation of the steps of the composite preparation process.

cells on 96-well plates using a cell density of  $10^5$  cells  $\text{ml}^{-1}$ . These cells were exposed to a control or test stock solution for 24 and 96 h in a  $\text{CO}_2$  incubator at  $37^\circ\text{C}$ . Subsequently, images were captured for cells treated with a higher stock solution concentration ( $100 \mu\text{g ml}^{-1}$ ) using phase contrast microscopy. After successful incubation, the culture medium was replaced with  $20 \mu\text{l}$  of  $2.5 \mu\text{g ml}^{-1}$  MTT salt solution in MEM media, followed by 4-h incubation. Then,  $50 \mu\text{l}$  of DMSO was added to dissolve the formazan dye. Absorbance was measured at 450 nm within 1 h using a SpectraMax M2e microplate reader. Control readings were represented as full cell survival (100% survival), and cell viability was calculated as a percentage using the following equation (1),

$$\% \text{ Cell viability} = \frac{\text{OD of test}}{\text{OD of control}} \times 100, \quad (1)$$

where OD stands for optical density, which is the absorbance reading.

### 3. Results and discussion

#### 3.1 Structural characterization

**3.1a Morphological characteristics by using XRD:** Figure 2 shows the diffractograms of pure UHMWPE and nanocomposites filled with 1, 5 and 10% HNT after compression moulding for  $2\theta$  values from 10 to  $80^\circ$ , the crystallinity percentage was also included. XRD has been used

to determine the dispersibility of nanoclay particles in UHMWPE/HNT nanocomposites by calculating the basal plane separation ( $d$ -spacing) based on Bragg's law, shown in equation (2),

$$d = \frac{n\lambda}{2\sin\theta}, \quad (2)$$

where  $\lambda$  is the X-ray wavelength,  $d$  the basal plane separation, and  $\theta$  the scattering angle [30]. The XRD pattern of HNT shows the major reflections at  $2\theta = 11.77$ ,  $20.068$ ,  $24.887$  and  $35.068$  corresponding to the planes at (001), (100), (002) and (110), respectively. As shown in figure 2, the diffraction patterns of the UHMWPE nanocomposites exhibited no diffraction of any characteristic peaks from  $10^\circ$  to  $21^\circ$ . This indicates the intercalation of UHMWPE molecular chains into the HNT spaces within the crystalline structure of nanoclay [30–32].

XRD phase analysis reveals that the UHMWPE consists of three main peaks belonging to an orthorhombic structure of polyethylene. These peaks situated at  $2\theta = 21.521^\circ$ ,  $2\theta = 23.938^\circ$  and  $2\theta = 36.302^\circ$  can be attributed to the (110), (020) and (200) lattice plane of the orthorhombic crystal with a preferred orientation plane of (110). The values of these peaks are consistent with the reported values of polyethylene [33–36]. In the fabricated nanocomposites, the prominent (110) peak of UHMWPE remained at the same position with 1 and 10% HNT and shifted to a lower angle for nanocomposites with 5% HNT. This suggests that basal  $d$ -spacing increased from 4.126 to 4.180 Å after adding 5% HNT, but unchanged from 4.126 Å after adding 1 and 10% HNT.

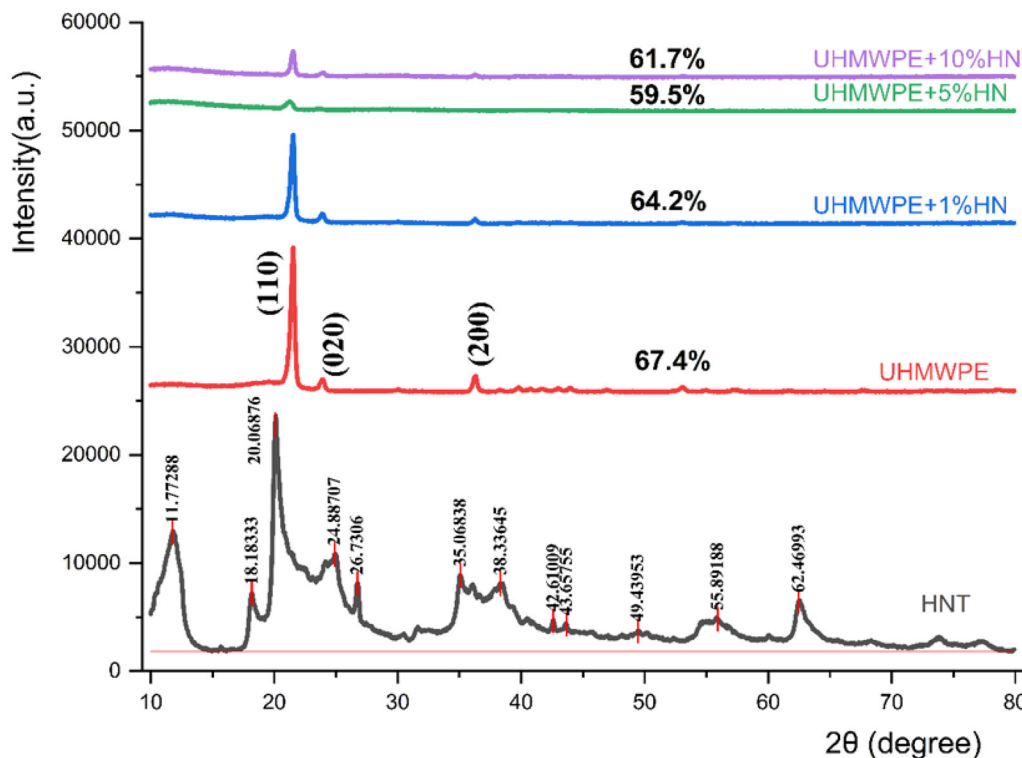


**Figure 2.** XRD patterns of HNT powder, pure UHMWPE and UHMWPE/HNT nanocomposites.

The position of (020) peak  $2\theta = 23.938^\circ$  changed to a lower angle  $2\theta = 23.881^\circ$  and  $2\theta = 23.600^\circ$  that caused an increased crystal spacing compared to pure UHMWPE from 3.714 to 3.723 Å and 3.767 Å with 1 and 5% HNT, respectively. Increasing  $d$ -spacing refers to good interaction between the polymer and HNT, leading to the formation of intercalated nanocomposites. In contrast, in nanocomposites with 10 wt% of HNT, the (020) peak shifted to a higher position with decreasing  $d$ -spacing to 3.706 Å. This can be attributable to the poor dispersion caused by large nanoclay loading, as shown in table 1. The diffraction peak position of (200) plane

shifted from  $2\theta = 36.302^\circ$  to  $2\theta = 36.245^\circ$  causing increased basal  $d$ -spacing as compared to pure UHMWPE from 2.473 to 2.477 Å for 1 and 10% HNT. Meanwhile, no basal distance was detected for 5% HNT due to the disappearance of the (200) peak, indicating that exfoliated morphology was obtained, and the polymer was successfully able to penetrate between the clay platelets. This result shows that the HNT has been exfoliated in the UHMWPE to form nanometre-scale exfoliated composites. Furthermore, the XRD analysis was used to measure the crystallinity of pure UHMWPE and the fabricated UHMWPE nanocomposites by using equation (3).

**Table 1.** Parameters of the crystallographic planes (110), (020) and (200) of pure UHMWPE and nanocomposites.

Diffraction plane	Composition	$2\theta$ (degree)	Intensity	$d$ -spacing (Å)
(110)	Pure UHMWPE	21.521	13736	4.126
	UHMWPE + 1%HNT	21.521	8525	4.126
	UHMWPE + 5%HNT	21.240	1013	4.180
	UHMWPE + 10%HNT	21.521	2656	4.126
(020)	Pure UHMWPE	23.938	1579	3.714
	UHMWPE + 1%HNT	23.8814	1242	3.723
	UHMWPE + 5%HNT	23.6004	415	3.767
	UHMWPE + 10%HNT	23.994	675	3.706
(200)	Pure UHMWPE	36.302	1910	2.473
	UHMWPE + 1%HNT	36.245	739	2.477
	UHMWPE + 5%HNT	—	—	—
	UHMWPE + 10%HNT	36.245	466	2.477

$$XC\% = \frac{I_c}{I_a + I_c}, \quad (3)$$

where  $I_a$  and  $I_c$  are the integrated intensities of amorphous and crystalline peaks, respectively [36].

However, it is noted that there is a remarkable decrease in relative intensity of the peaks referring to (110), (200) and (210) planes in the nanocomposites with an increase in the content of HNT to the UHMWPE polymer, causing an indistinct change in the degree of crystallization. The intensity of the (110) peak in the state of pure UHMWPE reaches 13736 with a crystallinity percentage of 67.4%, and when 1 and 5% HNT are added, the intensity of nanocomposites decreases to 8525 and 1013 causing a reduction in the crystallinity degree to 64.2 and 57.5%, respectively. On the contrary, the intensity of nanocomposite for 10% HNT increased to 2079, resulting in increased crystallinity degree to 61.7% compared to the content of 5% HNT.

The peak magnitude for UHMWPE+1% HNT is the most noticeable, especially on the (110) plane, indicating the most significant growth of the crystallites along the (110) direction compared to other nanocomposites.

**3.1b Fractographic study through SEM morphology:** As evident from the SEM micrographs from figure 3a and b, irrespective of HNT content, the obtained UHMWPE/HNT composites were homogenous in terms of the uniform dispersion of HNT particles. However, the distribution of HNT within the UHMWPE caused forming a minor agglomeration, especially with 10% HNT. The fractured surface morphology of UHMWPE displays dominant features of ductile fracture. The presence of dimples and tearing with stretched microfibrils caused by a crazing mechanism indicates the ductile behaviour of deformation. For 1% HNT, figure 3c and d, the nanocomposite showed high ductile strain, which is represented by intense tear lines and localized crazing (plastic deformation), creating a rough fracture surface and thus increasing resistance to crack propagation under sudden loading. Distributed HNTs bridge the crack, which looks surrounded by a network of very fine lines (plastic deformation) that cross the extension of the crack, reducing the stress intensity at the crack tip, thus preventing its progress and enhancing the absorbed energy of nanocomposite. Figure 3e–h illustrates the fracture surfaces of UHMWPE with 5 and 10% HNT, the composites exhibited tear lines suggesting plastic deformation prior to fracture. The pull-out (stretching) of material (fibrils), localized crazing, hackles, stable cracks and agglomerates were found.

Despite the decrease in Izod strength, the exfoliated structure of nanocomposite with 5% HNT permits the filler to bridge effectively the crack path because of its high aspect ratio. Therefore, the morphology of the fracture surface is characterized by surface roughness, with signs of elongated and deflected cracks due to the absorbed energy

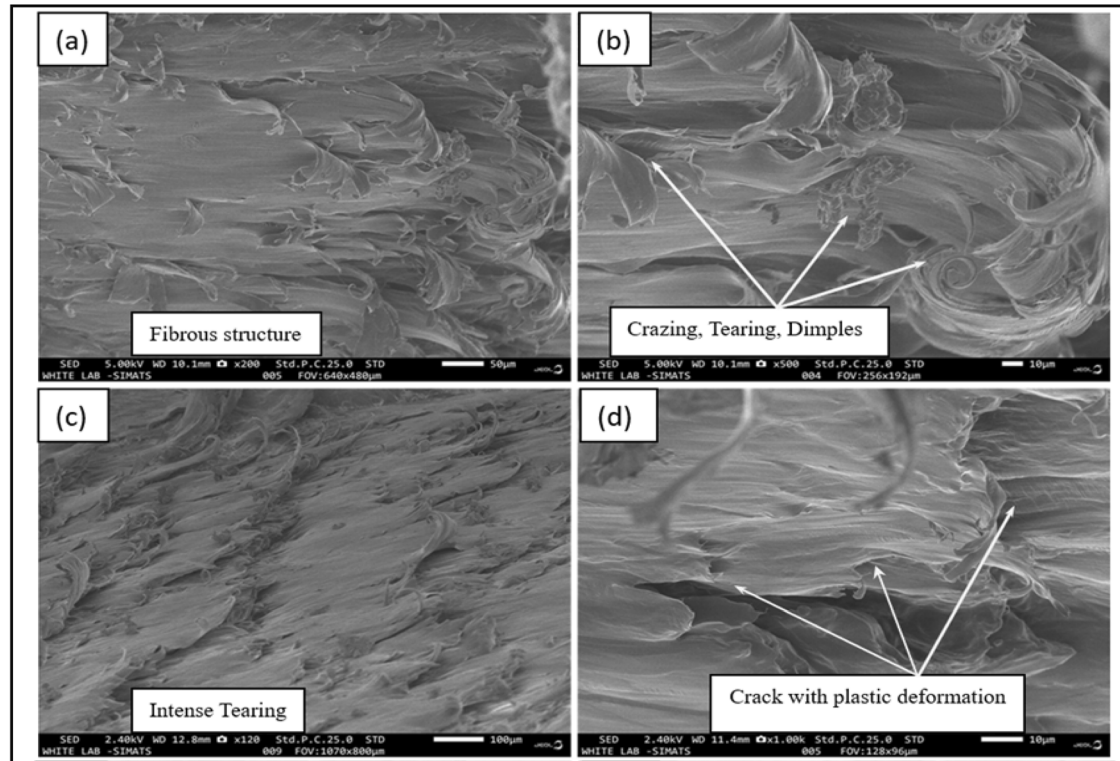
during deformation. As a result of this deviation, a feather-like region (hackles) is found, which indicates the stretching of HNT in the direction of crack propagation in a ductile manner, figure 3f. These hackles arise when the cracks propagate slowly through the matrix and are responsible for arresting an abrupt crack growth, thus lowering the amount of overall energy absorbed. The same mechanism was shown with 10% HNT. Notably, aggregations of HNT tend to increase in the matrix as the concentration of HNT increases. Meanwhile, the amount of plastic deformation reduced and appeared in the form of small fibrous extensions, especially with 10% HNT, figure 3g and h, causing a semi-ductile fractured structure. Consequently, the inclusion of HNT within UHMWPE exhibited a pronounced influence on impeding the advancement of cracks. Despite the drop in impact strength above 1% HNT, HNT served effectively as a mitigating mechanism to avoid the occurrence of catastrophic material failure.

### 3.2 Assessment of the bulk and surface mechanical properties

It was necessary to study the mechanical properties of specimens to ensure the relevancy of the material in THA and other orthopaedics applications. The following mechanical tests have been carried out to investigate properties including compression, abrasion, hardness, impact test and biocompatibility of UHMWPE/HNT composite.

**3.2a Hardness (shore D) measurements:** Several mechanical tests were conducted to assess the properties of the synthesized nanocomposites. Shore D hardness was measured on ten different points by using The Blue Steel SHR D GOLD tester according to ASTM D 2240. Abrasion resistance was performed on the Taber Rotary Platform Abrasion Tester Model 503 according to ASTM D 1044, using specimens ( $100 \times 100 \times 3.2 \text{ mm}^3$ ). A compression test was applied at specimens ( $12.7 \times 12.7 \times 25.4 \text{ mm}^3$ ) based on ASTM D695 using an Instron 3382 machine under constant speed at 25°C. To evaluate impact strength, the Izod notched test was carried out as per ASTM D 256, using notched samples ( $63.5 \times 12.7 \times 3.2 \text{ mm}^3$ ) with a 45-degree angle and 2.5 mm depth. The shore D hardness test results of unfilled UHMWPE and its nanocomposites with HNT are tabulated in table 2 and shown in figure 4. Overall, there was an improved hardness of pure UHMWPE after adding the HNT additives in all the fabricated nanocomposites regardless of their ratio. The enhancement of hardness values was more pronounced for small loading (up to 5 wt%) of HNT, especially for 5% where the greatest hardness increased to 73.5 by 29.1% as compared to unloading UHMWPE. This is due to the exfoliated structure of polymer chains in between two sheets of nanoclay (HNT). Herein, the high surface ratio of nano-filler can provide

(A)



(B)

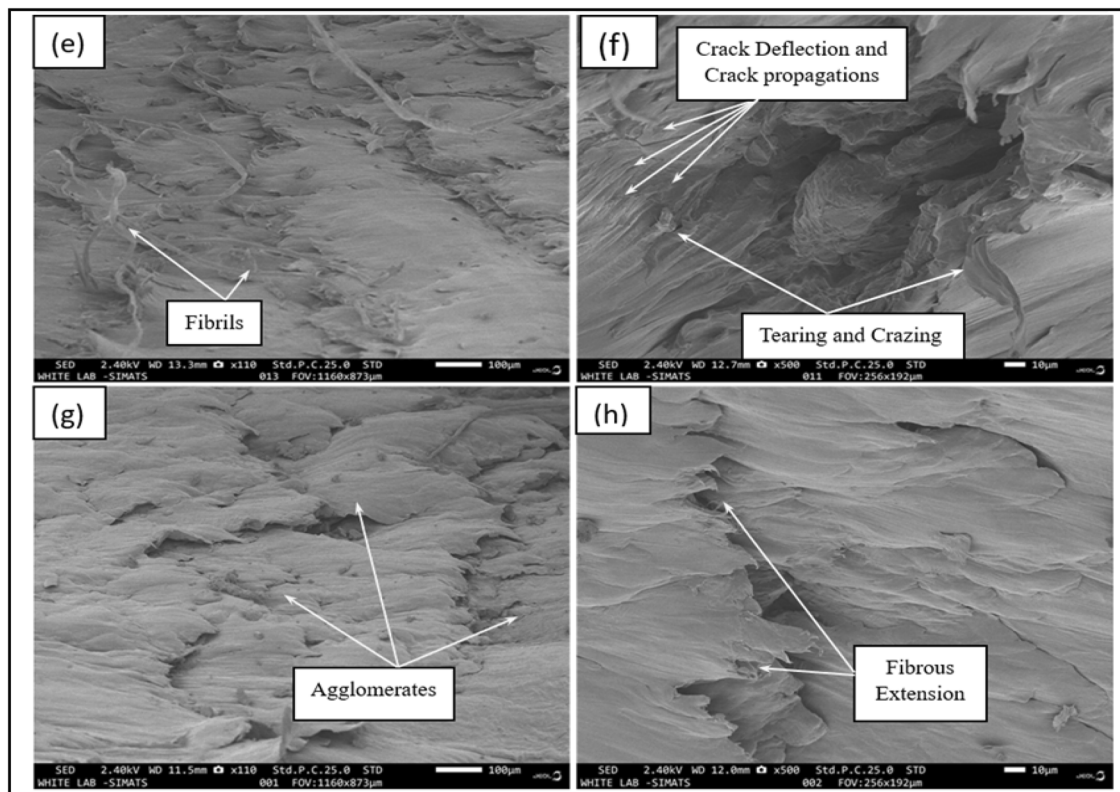


**Figure 3.** (A and B) SEM images of surface fractography of Izod fractured surface: (a, b) UHMWPE, (c, d) UHMWPE/1%HNT; (e, f) UHMWPE/5%HNT and (g, h) UHMWPE/10%HNT.

**Table 2.** Effect of HNT loading on impact Izod strength, hardness, wear loss and compressive properties of UHMWPE and their nanocomposites.

HNT (%)	Max. load (Kgf)	Strain at max. load (%)	Ultimate compr. strength (MPa)	Bulk modulus (MPa)	Izod energy absorption (kJ m <sup>-2</sup> )	Hardness (shore D)	Mass loss (g)
0	475.17	33	30.75	222.49	83.24 ± 8.97	57.1 ± 4.46	0.0183 ± 0.004
1	1446.80	79.4	84.47	301.55	92.69 ± 5.50	72.4 ± 2.57	0.0145 ± 0.0032
3	2088.25	72.13	127.83	435.75	68.89 ± 4.74	73 ± 3.47	0.0136 ± 0.0025
5	3730.55	81.00	221.08	1062.10	58.06 ± 4.89	73.5 ± 2.49	0.0122 ± 0.003
7	685.46	40.322	43.93957	280	83.47 ± 3.74	72.3 ± 3.35	0.0167 ± 0.0027
10	560.382	34.931	35.92	232.47	66.58 ± 6.57	72.1 ± 4.87	0.018 ± 0.0034

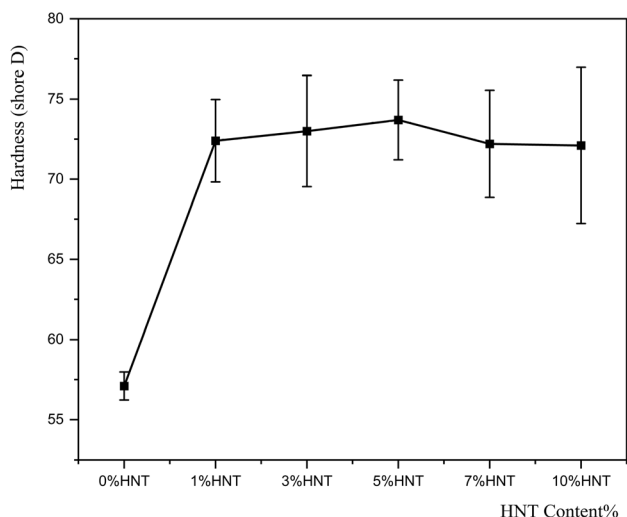


**Figure 4.** Hardness test of UHMWPE and composites as a function of HNT content.

excellent resistance towards indentation making the surface of the nanocomposite very hard. Above 5% HNT loading, the further weight fraction of HNT 7 and 10% HNT declines the indentation hardness values of nanocomposites to 72.2 and 72.1, respectively, due to poor dispersion and HNT aggregates. However, the deteriorated hardness of nanocomposites with 7 and 10% HNT remained effectually higher than the pure UHMWPE.

**3.2b Abrasion resistance:** A material’s ‘abrasion resistance’ refers to its ability to withstand the wear deformation caused by friction and repeated contact with other surfaces. If the material loses less of its surface quality under abrasive interactions, it demonstrates superior performance in terms of durability against abrasion. Basically, the lower the abrasion loss values, the better the material can withstand the test of time when subjected to wear, making it a desirable choice for more long-lasting applications. It is well known that surface hardness has a vital influence on the wear resistance of the composites. Accordingly, as can

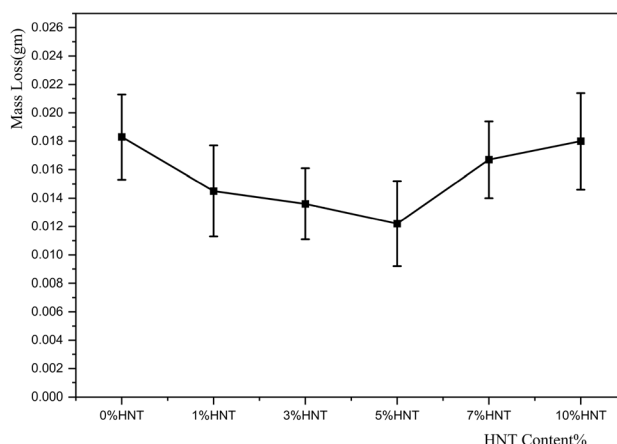


**Figure 5.** Mass loss vs. HNT loadings for pure UHMWPE and nanocomposites.

be seen from figure 5, the gradual reduction in abrasion-loss values was observed with an increase in loading of nanoclay up to 5% HNT, where the maximum average mass loss was from 0.0183 g for unfilled UHMWPE to 0.0122 g, thus enhancing the abrasion resistance of nanocomposite by 33.33%. Further reinforced by 7 and 10% of HNT, the nanocomposites experienced an increase in the abrasion-loss as compared to 5% of HNT by ~37 and ~47.5%, respectively. Well, these values remained lower than unfilled UHMWPE by 8.74 and 1.64%, suggesting that the abrasion resistance of nanocomposites was more effectively enhanced at lower levels of HNT, particularly with 5% HNT, where the pronounced abrasion durability was promoted.

**3.2c Compression test:** We have used MS Excel’s trend analysis feature to calculate bulk modulus based on the linear segments of a stress–strain curve in the elastic domain.

Based on the mechanical data collated in table 2, the stiffening attribute of the HNT nanotube and its interaction with the polymer matrix influenced the increase in

compressive properties of the final nanocomposites, irrespective of the percentage of HNT, when compared with unfilled UHMWPE.

As is clear from the figure and table, the mechanical properties of the nanocomposites were influenced by the amount of HNT filler in UHMWPE matrix. The response of the fabricated nanocomposites under the applied compressive load showed distinct behaviour in the stress–strain curve according to the loading percentage of the HNT nanotube. Firstly, for the small loading of HNT, when the percentage of HNT increased from 1 to 5 wt%, the stress–strain curve exhibits elastomeric behaviour (figure 6). These nanocomposites are characterized by a steady increase in the range of the plateau region of the stress–strain curve where the material undergoes plastic deformation without a significant increase in stress, followed by the strain-hardening region (where the material exhibits a significant increase in stress as it undergoes further deformation) during the compressive loading. From this region, the slope of the linear portion of the curve is identified, referring to the strain-hardening modulus, which determines how much the material will be strengthened as it is strained.

The incorporation of HNT into UHMWPE led to an augmentation in the interfacial stiffness and static adhesion strength of the nanocomposites, surpassing those of the unfilled polymer. This enhancement significantly facilitated the transmission of elastic deformation. Already after incorporating 1% of HNTs, the compressive strength and modulus increased by 174.7 and 35.5%, respectively, compared to the unfilled UHMWPE matrix reflecting an improved bonding strength at the interfaces of polymer and HNT nanoparticles. The compressive strength and modulus reached up to  $\sim 315$  and  $\sim 95\%$  with the introduction of 3% of HNT in UHMWPE. The largest increment in

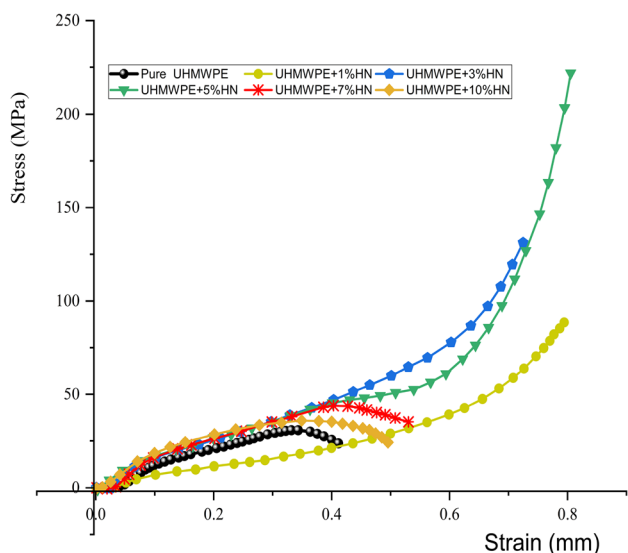


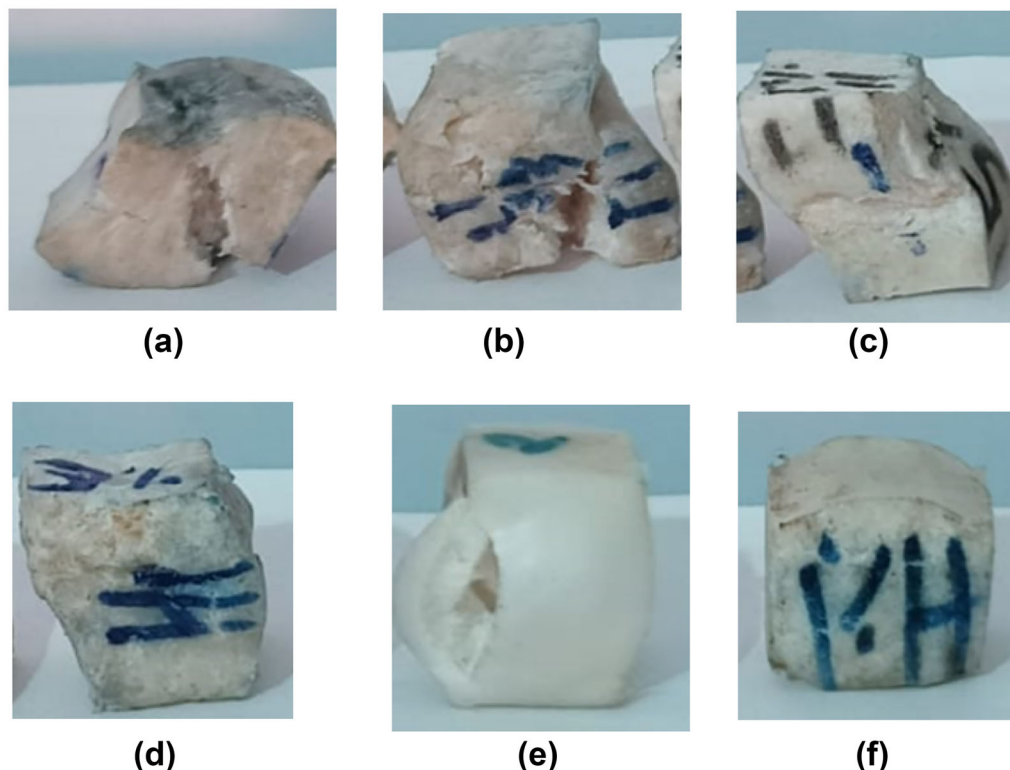
**Figure 6.** Stress–strain curve of pure UHMWPE and UHMWPE/HNT nanocomposites.

compressive strength and modulus of 221.08 and 1062.1 MPa were obtained with 5% loading of HNT. This pronounced enhancement in compressive strength and modulus amounted to  $\sim 617$  and  $\sim 377\%$  compared to corresponding values for unfilled UHMWPE. These findings imply that HNT demonstrates superior enhancing properties for UHMWPE when compared to CNT [37]. It can be seen from figure 5 that the compressive data of 1, 3, 5% HNT/UHMWPE nanocomposites are enhanced due to their drastically high ductility coming from high compressive strain ( $>70\%$ ), which never reduced with increasing stiffness. This distinct ductility was reflected in the appearance of damage mode in all nanocomposites; as seen in figure 7, the elastomeric nanocomposites experienced huge plastic deformation, allowing them to continue to deform permanently under high compression load without any fracture (only bulging) in 1% HNT and with local buckling (lateral deformation) for 2 and 3% HNT unlike UHMWPE, whose fracture surface showed a strong crack along the lateral edge due to buckling.

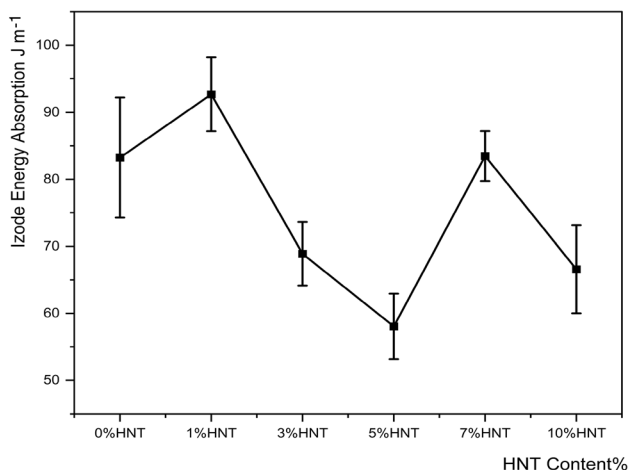
In the case of overloading above 5 wt%, the addition of 7 and 10% HNT into UHMWPE showed decreased compressive strength by  $\sim 81$  and  $83\%$ , and decreased compressive modulus by  $\sim 7$  and  $8\%$ , respectively, as compared to 5% HNT. However, the values of stress at break of nanocomposites containing 7 and 10% HNT, remained slightly over than the unfilled UHMWPE. In turn, the failure mode of nanocomposites after incorporation of 7 and 10% HNT into UHMWPE occurred under the influence of buckling and cracking as the failure mode of UHMWPE, but with less damage. Although the addition of HNT does enhance the compressive properties of the nanocomposite, it does not entirely prevent damage. This was due to the 7 and 10% HNT increase in the likelihood of agglomeration resulting from inadequate dispersion of the nanofiller in the polymer matrix. Eventually, in the case of small loading (less than 5%), the introduction of HNT further significantly reinforced UHMWPE in the case of high loading (above 5%). Hence, it might be concluded that 5 wt% HNT is the optimum weight percentage, which, if exceeded, will achieve less improved compressive strength and modulus as compared with small reinforcing (1, 3, 5%).

Figure 8 depicts a comparison between the Izod-notch impact strength of all nanocomposites and pure UHMWPE. After incorporating HNT into UHMWPE, different trends in Izod impact strength were observed. A very small increase in Izod impact strength was measured in the cases of 1 and 7% HNT reinforcement ( $\sim 11$  and  $0.285\%$  increase), respectively, compared to unfilled UHMWPE. Conversely, there was a remarkable reduction in Izod strength where the stiffness increased. Thus, the maximum reduction in Izod strength was noticed with 5% HNT ( $\sim 30\%$  decrease). However, further filling of HNT with 10 wt% diminished the notched strength by 15%. This might be caused by agglomerates of HNTs.





**Figure 7.** Damage modes of compression specimens for unfilled UHMWPE and HNT/UHMWPE nanocomposites: (a) UHMWPE+10% HNT, (b) UHMWPE+7% HNT, (c) UHMWPE+5% HNT, (d) UHMWPE+3% HNT, (e) UHMWPE+1% HNT and (f) UHMWPE+1% HNT.



**Figure 8.** Izod energy absorption as a function HNT content of UHMWPE and nanocomposites.

Although there are significant differences in the notched impact strength for manufactured nanocomposites, the failure mode of notched specimens exhibited either resistance to microcracking, where samples showed improved toughness (hinged break), or propagation of cracks from the notch and along the body of the specimen, where the notched strength was reduced. Nonetheless, there was no completed breakage

of any prepared nanocomposite under the Izod test. This implies the withstanding of prepared nanocomposites of significant deformation and stress before failing.

### 3.3 Nanocomposite result for biocompatibility in vitro

Figure 9a and b shows the percentage of cell viability of pure UHMWPE and their nanocomposites with 1, 5, 10% HNT after 1 day and 4 days of incubation at the three different concentrations of the test solution. The obtained results confirmed that all cells remained safe and viable, whether after 1 day or 4 days of incubation under the three different concentrations for all ratios of HNT. The results discovered that the longer exposure to the test solution after 4 days caused a slight reduction in cell viability for most samples and concentrations, the minimum percentage of cell viability was 94.307% with 10% HNT at 50 mg l<sup>-1</sup>, which inevitably indicates a high level of biocompatibility. Consequently, it can be said that HNT was appropriate for the MG-63 cells to proliferate at a high rate. When comparing the adsorption on the HNT/UHMWPE nanocomposites to that on the pure UHMWPE, there were no discernible differences, suggesting that the addition of HNT to UHMWPE had no detrimental effects on cell growth. This can be attributed

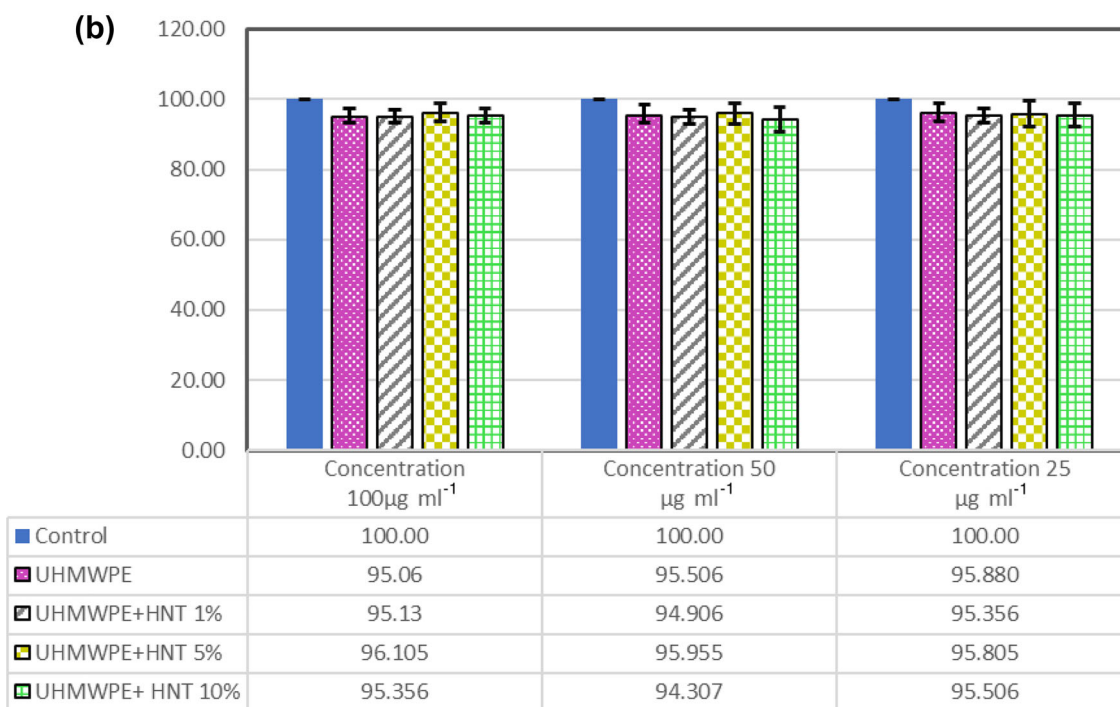
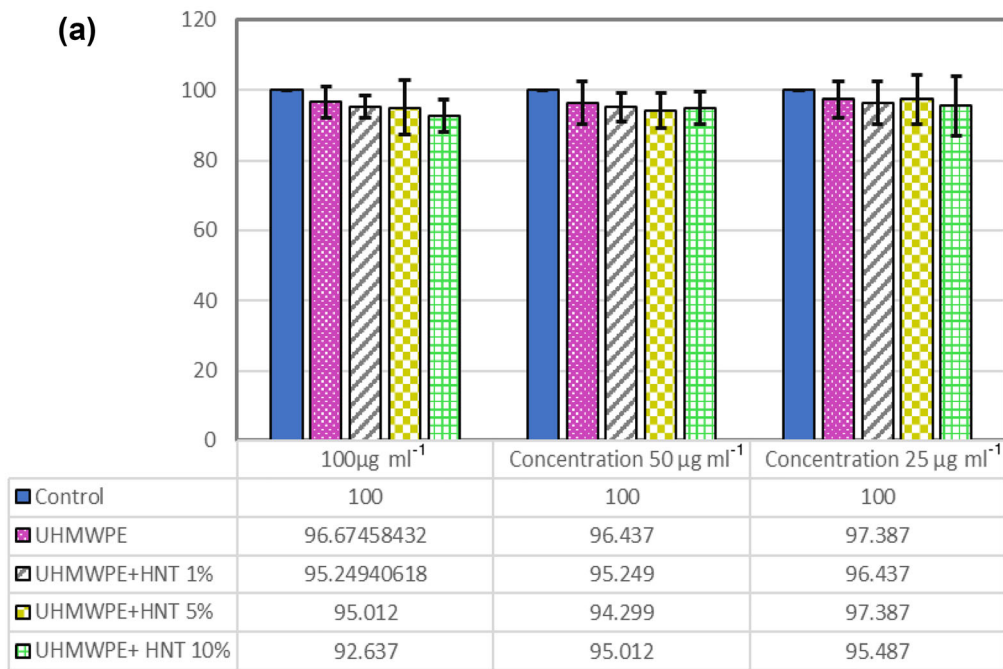


**Figure 9.** Influence of HNT ratios (1, 3 and 5%) on viability of MG-63 osteoblast at 100, 50 and 25 µg ml<sup>-1</sup> (a) after 1 day of incubation and (b) after 4 days of incubation.

to the excellent intrinsic biocompatibility of HNT that has been reported in the literature to be promising in medical applications.

Figure 10 displays that the cell viability exhibits excellent growth without any abnormalities at 100 µg ml<sup>-1</sup> after 4 days of incubation. Their morphology

remained intact with unchanged, and there were no indications of cytotoxicity when observed under a microscope despite the biocompatibility of HNT/UHMWPE nanocomposites consistently improved with all ratios. In this scenario, it is possible to further enhance the content of HNT by reducing it to less than 5%,

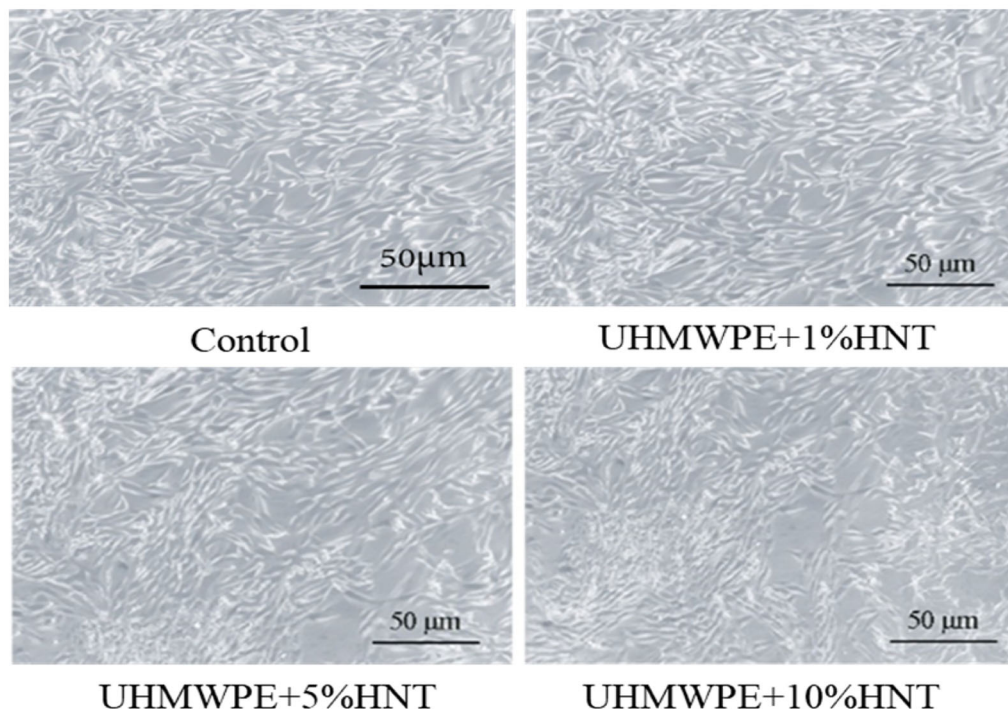


**Figure 10.** Optical images of osteoblast (MG-63) cells after 96 h incubation with  $100 \mu\text{g ml}^{-1}$  of test solution for 1, 3 and 5% of HNT.

ensuring better biocompatibility without compromising mechanical properties.

#### 4. Conclusion

In this study, the UHMWPE was successfully fabricated by two-roll milling and direct compression moulding with different percentages of HNT (1, 3, 5, 7 and 10%) and 5 wt% MA, which is used as a compatibilizer to achieve a well-dispersion nanostructure. SEM micrographs and XRD were adopted to characterize the fabricated UHMWPE/HNT nanocomposites. With the aim of application in orthopaedic implants, compression strength, impact Izod strength, surface hardness, abrasion resistance and biocompatibility were evaluated as critical parameters that dictated the selection of a joint. XRD analysis showed the intercalated, exfoliated and aggregated morphologies of HNT/UHMWPE nanocomposites detected with 1, 5 and 10% HNT, respectively. SEM analysis revealed the tendency of HNT to form clusters (agglomerates) with increasing HNT. However, HNT successfully bridged the crack advancement, preventing a catastrophic failure of the nanocomposite. Notched Izod strength showed a decrease in energy absorption compared to pure UHMWPE except 1% HNT, which experienced enhanced impact strength by 11.35%. The hardness shore D, abrasion resistance and compressive properties of UHMWPE/HNT were improved as compared to pure UHMWPE for all percentages and increased with increasing HNT. The results revealed that

there was an optimal limit of HNT (5 wt%), beyond which the evaluated properties were reduced. By MTT assay, the addition of HNT to UHMWPE showed a positive effect in terms of cell viability, as a result osteoblast (MG-63) cells exhibited no signs of cytotoxicity. This moreover, proliferated after incubation for 24 and 96 h in a cultured medium containing different concentrations ( $100$ ,  $50$  and  $25 \mu\text{g ml}^{-1}$ ) of prepared test solutions. In light of these results, UHMWPE/HNT promoted interestingly the fundamental properties that are essential for load bearings used in artificial joint replacements.

#### Acknowledgements

We acknowledge CIPET Ahmedabad for creating compounding and plastic testing facilities. We are thankful to Saveetha Dental College, Chennai, for XRD and SEM facility, and Saurashtra University, Rajkot, for the biocompatibility test. We are also thankful to Marwadi University for its infrastructural facility.

#### References

- [1] Burger N D L, de Vaal P L and Meyer J P 2007 *Eng. Fail. Anal.* **14** 1329
- [2] Evans S L and Gregson P J 1998 *Biomaterials* **19** 1329
- [3] Ramakrishna S, Huang Z M, Kumar G V, Batchelor A W and Mayer J 2004 *An introduction to biocomposites* (London: Imperial College Press) p 175

- [4] Mohammed M T 2019 *Applications of nanocomposite materials in orthopaedics* (Cambridge: Woodhead Publishing) p 221
- [5] Hussain M, Naqvi R A, Abbas N, Khan S M, Nawaz S, Hussain A *et al* 2020 *Polymers* **12** 323
- [6] Patil N A, Njuguna J and Kandasubramanian B 2020 *Eur. Polym. J.* **125** 109529
- [7] Guofang G, Huayang Y and Xin F 2004 *Wear* **256** 88
- [8] Dangsheng X 2005 *Mater. Lett.* **59** 175
- [9] Bhaskar B, Arun S, Sreekanth P and Kanagaraj S 2016 *Trends Biomater.* **5** 175
- [10] Affatato S 2014 *Perspectives in total hip arthroplasty* (Cambridge: Elsevier Publishing) p 19
- [11] Black J 1988 *Ortho. Biomater. Res. Prac.* **1** xix
- [12] Singh R K and Gangwar S 2021 *Int. J. Eng. Sci. Tech.* **13** 25
- [13] Aherwar A, Singh A K and Patnaik A 2015 *AIMS Bioeng.* **3** 23
- [14] Puértolas J A and Kurtz S M 2016 *UHMWPE Biomaterials handbook* (Netherlands: Elsevier Inc.) p 369
- [15] Fang L, Leng Y and Gao P 2006 *Biomaterials* **27** 3701
- [16] Fang L, Gao P and Leng Y 2007 *Compos. B Eng.* **38** 345
- [17] Lahiri D, Dua R, Zhang C, Socarraz-Novoa I D, Bhat A, Ramaswamy S *et al* 2012 *ACS Appl. Mater. Inter.* **4** 2234
- [18] Taromsari S M, Salari M, Bagheri R and Faghihi Sani M A 2019 *Compos. B Eng.* **175** 107181
- [19] Singh D K and Verma R 2023 *J. Therm. Compos. Mater.* **36** 3516
- [20] Jacobs O and Schädel B 2008 *Tribol. Interface Eng. Series* **55** 209
- [21] Zou Y, Feng Y, Wang L and Liu X 2004 *Carbon* **42** 271
- [22] Zhang Y, Ali S F, Dervishi E, Xu Y, Li Z, Casciano D *et al* 2010 *ACS Nano* **4** 3181
- [23] Liu S, Zeng T H, Hofmann H, Burcombe E, Wei J, Jiang J *et al* 2011 *ACS Nano* **5** 6971
- [24] Massaro M, Noto R and Riela S 2020 *Molecules* **25** 4863
- [25] Kamble R, Ghag M, Gaikawad S and Panda B K 2012 *J. Adv. Sci. Res.* **3** 25
- [26] Biddeci G, Cavallaro G, Blasi F D, Lazzara G, Massaro M, Milioto S *et al* 2016 *Carbo. Poly.* **152** 548
- [27] Maisanaba S, Pichardo S, Puerto M, Praena D G, Cameán A M and Jos A 2015 *Environ. Res.* **138** 233
- [28] Krepker M, Shemesh R, Poleg Y D, Kashi Y, Vaxman A and Segal E 2017 *Food Control* **76** 117
- [29] Shutava T G, Fakhrullin R F and Lvov Y M 2014 *Curr. Opin. Pharmacol.* **18** 141
- [30] Chen H D, He Y W and Zhang W 2005 *Compos. Sci. Tech.* **65** 1593
- [31] Barakat M A, Kumar R, Balkhyour M and Taleb M A 2019 *RSC Adv.* **9** 13916
- [32] Cavallaro G, Lazzara G and Milioto S 2011 *Langmuir* **27** 1158
- [33] Chagas N P, Aguiar V O, Garcia Filho F C, Figueiredo A B H, Monteiro S N, Huaman N R C *et al* 2022 *J. Mater. Res. Tech.* **17** 1799
- [34] Abdalsalam A H, Sayyed M I, Hussein T A, Şakar E, Mhareb M H A, Şakar B C *et al* 2019 *Chem. Phys.* **523** 92
- [35] Chouit F, Guellati O, Boukhezar O, Harat A, Guerioune M and Badi N 2014 *Nano Res. Lett.* **9** 1
- [36] Guan C, Yang H, Li W, Zhou D, Xu J and Chen Z R 2014 *J. Appl. Polym. Sci.* **131** 40847
- [37] Kharitonov A P, Maksimkin A V, Mostovaya K S, Kaloshkin S D, Kaloshkin M V, Gorshenkov M V *et al* 2015 *Compos. Sci. Tech.* **120** 26

Springer Nature or its licensor (e.g. a society or other partner) holds exclusive rights to this article under a publishing agreement with the author(s) or other rightsholder(s); author self-archiving of the accepted manuscript version of this article is solely governed by the terms of such publishing agreement and applicable law.